

# THE BRITTLE TENSILE FRACTURE AND CLEAVAGE STRENGTH OF A STRUCTURAL STEEL WITH A SIMULATED WELD-AFFECTED-ZONE MICROSTRUCTURE

## TRDNOST PRI KRHKEM PRELOMU IN CEPILNA TRDNOST ZA KONSTRUKCIJSKO JEKLO S SIMULIRANO MIKROSTRUKTURO TOPLOTNE CONE ZVARA

Gorazd Kosec<sup>1</sup>, Boris Arzenšek<sup>2</sup>, Jelena Vojvodič Tuma<sup>2</sup>, Franc Vodopivec<sup>2</sup>

<sup>1</sup>SIJ, d. d., Acroni, d. o. o., Kidričeva 44, 4270 Jesenice, Slovenia

<sup>2</sup>Institute of Metals and Technology, Lepi pot 11, 1000 Ljubljana, Slovenia  
gorazd.kosec@acroni.si

*Prejem rokopisa – received: 2008-11-13; sprejem za objavo – accepted for publication: 2008-12-23*

Tensile tests were carried out on specimens of the same micro-alloyed structural steel after different thermal treatments, with the aim being to obtain the microstructure in a weld's heat-affected zone. The mechanical properties were determined at a temperature below the brittle threshold transition Charpy temperature, the fracture surfaces were examined, the cleavage strength was deduced and the space orientation of the cleavage facets was determined. No relation was found between the results of the tensile tests and the previously determined Charpy properties after an identical thermal treatment.

Key words: micro-alloyed structural steel, cleavage strength, fracture surface morphology, cleavage facet orientation

Opravili smo raztržne preizkuse mikrolegiranega konstrukcijskega jekla, ki je bilo toplotno obdelano za dosego nekaterih mikrostruktur v toplotni zoni zvara. Določili smo mehanske lastnosti pri temperaturi pod pragom krhkega Charpyjevega preloma, pregledali prelomne površine, izračunali cepilno trdnost in določili prostorsko orientacijo cepilnih ploskev. Našli nismo nobene povezave med rezultati te raziskave in značilnostmi Charpyjevega preloma jekla po enaki toplotni obdelavi.

Ključne besede: mikrolegirano konstrukcijsko jeklo, cepilna trdnost, značilnosti krhkega preloma, prostorska orientacija cepilnih ploskev

## 1 INTRODUCTION

With the aim being to explain the difference in the Charpy toughness transition temperatures of the welds in steel plates of different thicknesses from the same structural steel with a yield stress of 490 MPa, the transition temperature was determined for ten types of microstructure: the initial microstructure of fine-grained tempered martensite, the coarse- and fine-grained primary martensite and bainite, the coarse- and fine-grained primary bainite and these basic microstructures with the secondary martensite obtained by reheating the specimens in the two-phase region – ferrite+ austenite – and air cooling<sup>1</sup>. We found that after reheating the transition temperature was increased and the upper-shelf toughness decreased the most for the microstructure of bainite, especially for coarse-grained bainite<sup>1</sup>. These experimental findings confirmed the assumption that the coarse bainite microstructure was the most likely to form LBZs (local brittle zones) in the heat-affected zone of the welds<sup>1,2</sup>.

In this article we present and discuss the results of an investigation aimed to determine whether the transition temperature was related to the brittle tensile strength and

the cleavage strength of different microstructures, as quenched and after a reheat.

## 2 EXPERIMENTAL WORK

A fine-grained steel (0.11 C, 0.5 Mn, 0.54 Cr, 0.34 Mo, 0.014 Ti and 0.032 Nb) with an initial microstructure of tempered martensite and ferrite and a linear intercept length of 3  $\mu\text{m}$  was investigated. The specimens were quenched at 920 °C and 1250 °C in water at 70 °C or in a lead bath at 400 °C. To simulate the heat cycle during the deposition of the next welding pass, half of the specimens were submitted to reheating for 3 s at 750 °C and air cooling. All the tensile tests were performed on two parallel specimens with a circumferential notch with a shape and size the same as that used in the laboratory for determining the fracture toughness of tool steels with a low notch toughness<sup>3</sup>, and similar to those used for investigations of the cleavage strength of structural steels<sup>4,5,6</sup>. The diameter of the cylindrical part of the specimen was 10 mm, with a diameter of 8 mm in the notch. The cross-head speed was 5 mm min<sup>-1</sup> and the testing temperature was –120 °C, some 30 °C or more lower than the lower-shelf notch toughness threshold temperature<sup>7</sup>. Notched specimens

were used because for flat tensile specimens at approximately  $-130\text{ }^{\circ}\text{C}$ , some  $30\text{ }^{\circ}\text{C}$  lower than the nil ductility temperature, the steel exhibited ductile fracturing with a 65 % reduction of the area. However, with notched specimens the brittle fracturing was obtained already at  $-115\text{ }^{\circ}\text{C}$  <sup>8</sup>.

From the obtained dependences it was possible to determine the range of elastic and plastic deformation of the specimen before fracture, the elastic stress at the onset of plastic deformation and the fracture stress. The fractured surfaces were examined visually and on an SEM, and special care was given to the fracture micro-morphology along the notch tip, to the transition area and to the boundary area between the ductile ring and the brittle central area. The orientation of the brittle

facets was determined for some specimens with EBSD (electron back-scatter diffraction).

### 3 BRITTLE TENSILE STRENGTH AND EXTENT OF PLASTIC DEFORMATION

In **Figures 1 to 4** the characteristic recorded dependences of the tensile force versus the deformation are given: a case with the fracture virtually in the range of proportionality force-deformation in **Figure 1** (type A), two cases with an increasing extent of plastic deformation in **Figures 2 and 3** (type B) and a case with a clear yielding in **Figure 4** (type C). In **Table 1** the extent of the plastic deformation before the fracture (*PD*), the brittle tensile strength (*BFS*), the deduced value of the cleavage strength, the Vickers hardness, the width of the ring of plastic shearing at the notch tip as,

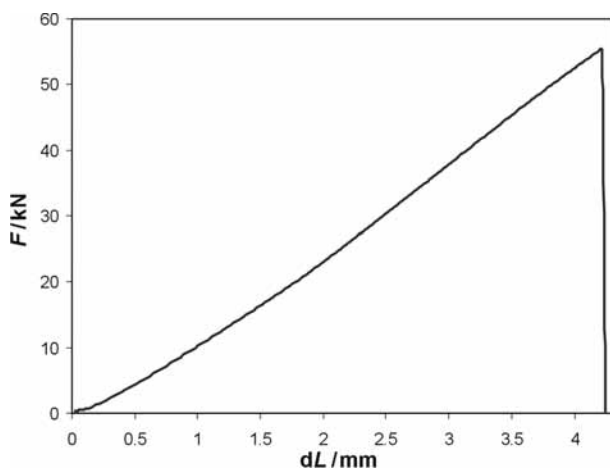


**Figure 1:** Dependence of force vs. extension for a specimen quenched from  $1250\text{ }^{\circ}\text{C}$  and reheated at  $750\text{ }^{\circ}\text{C}$ . Microstructure: coarse-grained tempered primary martensite and secondary martensite.

**Slika 1:** Odvisnost sila-podaljšek za preizkušane, kaljen v vodi s  $1250\text{ }^{\circ}\text{C}$  in segreti pri  $750\text{ }^{\circ}\text{C}$ . Mikrostruktura: popuščeni grobozrnati primarni martenziti in sekundarni martenziti

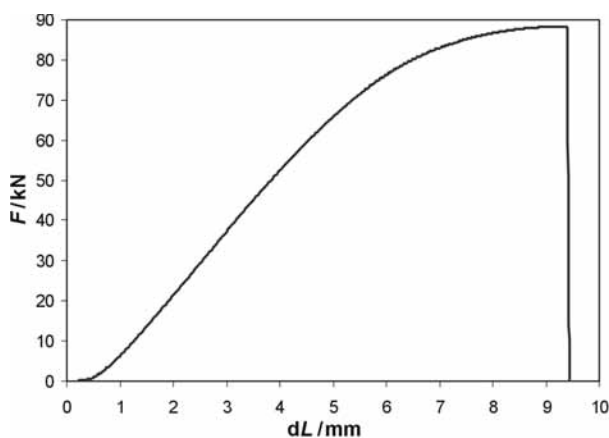


**Figure 3:** Dependence of force vs. extension for a specimen quenched in water from  $920\text{ }^{\circ}\text{C}$  (a). Microstructure: fine-grained martensite

**Slika 3:** Odvisnost sila-podaljšek za preizkušane, kaljen v vodi s  $1250\text{ }^{\circ}\text{C}$ . Mikrostruktura: drobno zrnati martenziti

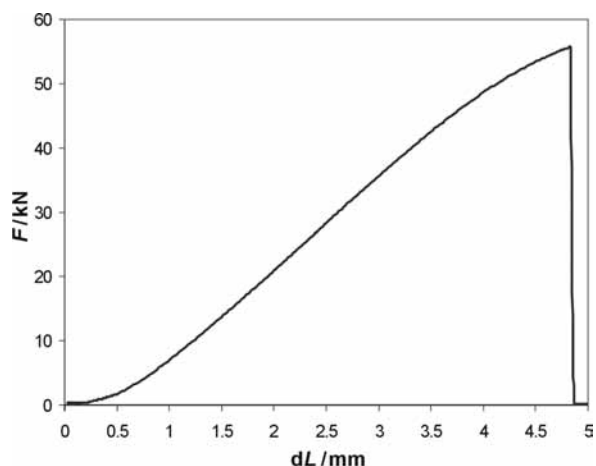


**Figure 2:** Dependence of force vs. extension for the specimen quenched from  $1250\text{ }^{\circ}\text{C}$  in a lead bath at  $400\text{ }^{\circ}\text{C}$  and reheated at  $750\text{ }^{\circ}\text{C}$ . Microstructure: coarse-grained bainite and secondary martensite

**Slika 2:** Odvisnost sila-podaljšek za preizkušane, ohlajeni v svincu s  $1250\text{ }^{\circ}\text{C}$  in segreti pri  $750\text{ }^{\circ}\text{C}$ . Mikrostruktura: grobozrnati bainit in sekundarni martenziti

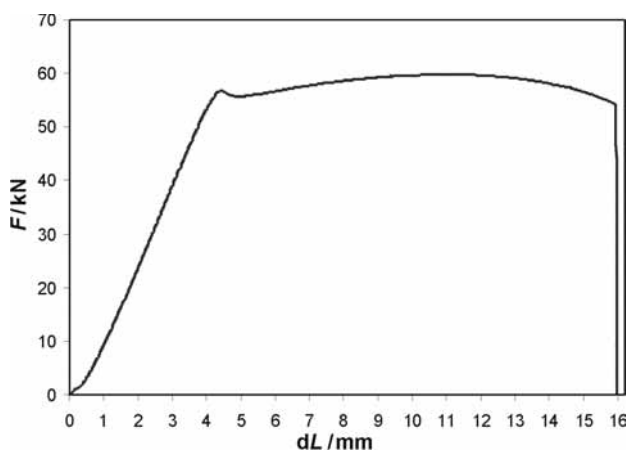


**Figure 4:** Dependence of force vs. extensions for a specimen with the initial microstructure reheated at  $750\text{ }^{\circ}\text{C}$ . Microstructure: fine-grained tempered martensite–ferrite and secondary martensite

**Slika 4:** Odvisnost sila-podaljšek za preizkušane z začetno mikrostrukturo, segreti pri  $750\text{ }^{\circ}\text{C}$ . Mikrostruktura: popuščena fino zrnati martenziti in ferit ter sekundarni martenziti

the Charpy fracturing energy at 0 °C (CV0) and the lower-shelf Charpy temperature-temperature of cleavage fracture (CVC) are given. In the discussion the characteristics of the specimen with the initial microstructure are used for the comparison.

The steel with the initial microstructure of tempered martensite shows the dependence force versus the extension (tensile curve) of the C type, a significant plastic extension and a reduction of the area of 8.1 %. After reheating at 750 °C, the hardness and the brittle tensile strength (*BFS*) are higher, the tensile curve is of the C type with clear yielding and the plastic extension is increased to 2.41 mm, while the reduction of the area is lowered to 3.7 %. The differences between both specimens are attributed to the presence of secondary martensite in the microstructure of the specimen reheated at 750 °C.

After water quenching from 920 °C the tensile curve is of the B type; the hardness and especially the *BFS* are greater than for the steel with the initial microstructure. As would be expected for the microstructure of quenched fine-grained martensite, the plastic extension is similar to that for the initial microstructure and the reduction of the area below the detection limit. After reheating, the type of the tensile curve is not changed; however, all the characteristics are lowered and indicate that the effect of tempering of the primary martensite exceeded the effect of the presence of secondary martensite. After water quenching from 1250 °C, the tensile curve is of the A type, the hardness is strongly increased, the *BFS* slightly, the plastic extension is at the detection limit and much lower than after quenching from 920 °C. After reheating, the type of tensile curve is not changed, the hardness is significantly lower, the *BFS* is slightly changed and the plastic extension is very low.

After cooling in a lead bath from 920 °C, the tensile curve is of the B type, the hardness is slightly higher, the *BFS* significantly increased and the plastic extension was virtually equal to that for the initial microstructure. After reheating the tensile curve is unchanged, the hardness is changed little and the *BFS* and the plastic extension are lower. After lead cooling from 1250 °C the tensile curve is of the B type, the hardness is unchanged, the *BFS* is slightly increased and the plastic extension slightly decreased. After reheating, the tensile curve is unchanged, the hardness is significantly higher, the *BFS* slightly lower and the plastic extension much lower.

The change of hardness reflects the characteristics of the microstructure and its changes after reheating. The hardness is increased more after water quenching and especially after quenching from 1250 °C. After reheating, the hardness is slightly higher for the specimens with the initial and bainite microstructures, while it is lower for the martensite microstructure. It is concluded that the softening effect of the tempering of primary martensite exceeds the effect of the presence of secondary martensite.

The brittle fracture strength (*BFS*) was very different for the different microstructures and in all cases, with the exception of the as-delivered microstructure, it was slightly lower after reheating. Somewhat surprisingly, after quenching from 1250 °C the hardness is increased more than the *BFS*, while after reheating the hardness is decreased and the *BFS* virtually unaffected.

These findings indicate that the reheating affects differently the Charpy properties, not only the transition temperature of the ductile-to-brittle fracture<sup>1</sup>, but also the hardness of the martensite and bainite and *BTS* and also show that the hardness is not related to the *BTS*. In comparison to the initial microstructure, the plastic extension is lower for all the other specimens, and it is especially low for the martensite obtained with water quenching from 1250 °C. After reheating it is higher for the initial microstructure and lower for all the other tested microstructures. These findings indicate that the hardness of the different microstructures in the weld-affected zone cannot be used as a reliable measure of the other properties of these microstructures.

#### 4 CLEAVAGE STRENGTH

The cleavage strength ( $E_{cl}$ ) depends on the brittle fracture strength (*BFS*) and on the specimen's geometrical shape. It is deduced from the nominal fracture stress ( $E_n$ ) considering the specimen ( $r_{ns}$ ) and the notch radius ( $r_n$ )<sup>8,9</sup>:

$$E_{cl}/E_n = 1 + \ln(1 + r_{ns}/r_n) \quad (1)$$

For notched specimens the real stress at the notch tip depends on the stress-concentration factor<sup>10</sup>  $K_p$ :

$$K_p = 1 + \ln(1 + R/r_c) \quad (2)$$

With  $R$  being the radius (extension of the plastic zone ahead of the crack notch) tip and  $r_c$  being the crack-tip radius. With instrumented Charpy tests the stress-concentration factor was, in the temperature range 60 °C to -20 °C, 3.22 to 3.35 for a 0.17 % C – 1.28 % Mn steel and 2.42 to 2.62 for the steel investigated<sup>11</sup>. This factor was termed as a ratio of the yield stress obtained with the Charpy instrumented tests and the yield stress of the tensile cylindrical specimens. Using the average value for the stress-concentration factor of 2.52 and the steel yield stress of 490 MPa a stress concentration of 1234 MPa is deduced. On notched specimens the brittle tensile strength of 1250 MPa was found for the investigated steel at<sup>12</sup>. Experimental findings show that the stress-concentration factor also depends on the properties of the steel that probably determine the acuity of the propagating crack tip. The crack tip radius is calculated as<sup>12</sup>:

$$r_c = 0.32 (E/E_{cl})\delta \quad (3)$$

or for a sharp crack:

$$r_c = (1/6\pi) (K_{IC}/E_{cl})^2 \quad (4)$$

**Table 1:** Characteristics of the tensile and Charpy notch tests and of the tensile fracture surfaces**Tabela 1:** Značilnosti raztržnega preizkusa, Charpyjevih preizkusov in raztržnih prelomov

Specimen	Hardness <i>HV</i> 5	<i>BFS</i> MPa	<i>CS</i> MPa	<i>PE</i> mm	<i>WDS</i> mm	<i>CT0</i> J	<i>CTT</i> °C
Initial	205	1063	1934	1.33	0.41	240	-100
" + 750 °C	249	1231	2240	2.41	0.37	95	-80
920 °C wat.	282	1449	2637	1.35	0.13	120	-100
" + 750 °C	244	1329	2402	0.65	0.07	50	-50
1250 °C wat.	383	1257	2287	0.23	0.07	45	-40
..." + 750 °C	320	1230	2238	0.11	0.06	20	-40
920 lead	222	1208	2198	0.97	0.09	250	-100
" + 750 °C	241	1106	2012	0.59	0.07	27	-20
1250 lead	204	1255	2284	0.82	0.11	205	-80
" + 750 °C	248	1052	1914	0.35	0.08	14	0

*BFS* – brittle fracture strength

*CS* – cleavage strength

*PE* – plastic extension

*WDS* – width of the ring of ductile shearing

*CT0* – Charpy notch toughness at 0 °C

*CTT* – Cleavage threshold temperature

with  $E$  equal to the elastic modulus,  $\delta$  being the crack-opening displacement and  $K_{IC}$  the fracture toughness.

In the transition zone of the ductile-to-brittle fracture of the fracture surface of the notched specimens fractured below the lower-shelf notch toughness threshold a layer of smaller dimples was observed that passed over to the cleavage area with an area of plane shearing<sup>12</sup>. In this investigation it was found that the cleavage crack extension did not start at the notch tip, but from an initial shearing crack started at the notch. This observation is in agreement with the finding<sup>13</sup> that the plastic yielding is a necessary precursor to the cleavage and that maybe slip or twinning is involved in the nucleation of a cleavage fracture. In this investigation a shearing ring was found on all the tensile fractures at the notch tip. Accordingly, it is assumed that the thickness of the plastic deformation layer ahead of the de-cohesion tip decreases gradually until a critical value of the notch tip radius ( $r_c$ ) is obtained, and that at this point the cleavage de-cohesion is initiated. For the value of the critical crack tip a radius of  $6.2 \cdot 10^{-8}$  m was calculated<sup>8</sup> using the modified equation (5)

$$r_c = (1/6\pi) (K_{IC}/E_{cl})^2 (d_c/d)^3 \quad (5)$$

Where  $d_c$  is the critical size of the dimples ahead of the ductile shearing layer and  $d$  is the dimples' size for ductile crack propagation.

It is necessary to stress that in our tests a significant plastic deformation occurred without clear yielding and the effect of the grain size on the cleavage strength was confirmed only for the martensite microstructure<sup>14,15</sup>.

In this investigation the specimen and the notch tip radius were 5 mm and 0.2 mm. Applying equation (1) the cleavage strength of  $E_{cl} = 1.82 E_n$  is deduced.

The cleavage strength in **Table 1** was deduced for every specimen considering the accurate diameter of the cylindrical specimen and the diameter of the fracture surface. In comparison with the initial microstructure, the cleavage strength is higher after reheating and for all the as-quenched microstructures, particularly for the martensite obtained with quenching from 920 °C. In all cases, except for the initial microstructure, the cleavage strength is lower after reheating. The explanation could be the internal stresses generated by the formation of secondary martensite. The cleavage strength is lower for both bainitic microstructures.

No indication was found for an eventual effect of plastic straining on the cleavage strength. Little of the energy is spent for the cleavage propagation, mostly for the displacement of the crack tip in the cleavage plane of the new grain with a different space orientation and less for the overcoming of the dislocations that generates river patterns on the cleavage surface. Thus, it is assumed that the presence of a greater number of dislocations generated by the plastic extension, that is different for different microstructures, did not significantly affect the value of the cleavage strength.

## 5 FRACTURE MORPHOLOGY AND ORIENTATION OF THE CLEAVAGE FACETS

The fracture surface of all the specimens consisted of a ring of shearing at the notch tip of different widths and a central area of cleavage (**Figure 5**). On all specimens two or even three crack initials were found in the notch tip (**Figure 6**) that joined rapidly in a ring of plane shearing. On this surface an increasing number of dimples were found at greater distances from the notch tip. At the boundary of the shearing ring, the fracture changed sharply to cleavage with facets, the size of



**Figure 5:** Fracture surface of a notched tensile specimen of steel quenched in water from 1250 °C. Microstructure: coarse-grained martensite

**Slika 5:** Prelomna površina razteznega preizkušanca, kaljenega v vodi s 1250 °C. Mikrostruktura: grobozrnati martenzit



**Figure 7:** Fracture surface of a notched tensile specimen cooled in a lead bath from 1250 °C. Microstructure: coarse-grained bainite

**Slika 7:** Prelomna površina razteznega preizkušanca, ki je bil ohlajen v svincu s 1250 °C. Mikrostruktura: grobozrnati bainit



**Figure 6:** Fracture surface of a notched tensile specimen quenched in water from 920 °C and reheated at 750 °C. Microstructure: tempered primary fine grained martensite and secondary martensite

**Slika 6:** Prelomna površina razteznega preizkušanca, ki je bil kaljen v vodi s 920 °C in segret pri 750 °C. Mikrostruktura: popuščeni finozrnati primarni martenzit in sekundarni martenzit

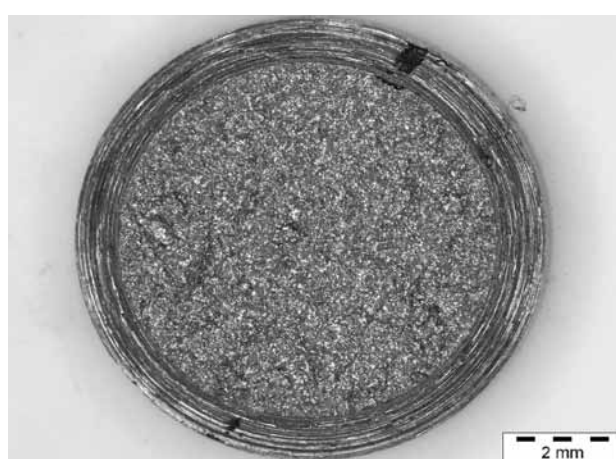


**Figure 8:** Cleavage surface of the steel cooled in lead bath from 920 °C. Microstructure: fine-grained bainite only

**Slika 8:** Cepilna površina jekla, ki je bilo ohlajeno v svincu s 920 °C. Mikrostruktura: drobnozrnati bainit

which depended on the austenite grain size before the quenching (**Figures 7 and 8**). No difference in the cleavage morphology is found that could be attributed to the presence of secondary martensite after reheating at 750 °C.

The width of the ring at the notch tip was different for different specimens. It was much greater for the steel with an initial and reheated microstructure that had a tensile curve of the type C with clear yielding and a greater plastic extension. For all the other specimens it was much smaller and even smaller after reheating. It is assumed that the ring consists partly of the layer of metal deformed at the cutting of the notch and partly of the shearing extension when the crack tip decreased to the size required for the change of propagation from shearing to cleavage. The different width also suggests

that the critical crack tip radius is not equal for all the investigated microstructures. Since the plastic extension and the shearing width ring are smaller for the as-reheated microstructures, with the exception of the initial microstructure, it is concluded that the internal stresses generated by the formation of a secondary martensite also affect the stress-concentration factor  $K_s$  and the critical crack tip radius given in equations (2), (3), (4) and (5).

The cleavage facets on the brittle fracture of a structural steel could have the space orientations (011) and (001)<sup>16</sup>. On some fracture surfaces an EBS diffraction was carried out to determine if the cleavage facets' spatial orientation was different for the different microstructures. To obtain a clear diffraction pattern, the angle between the specimen surface of the electron-collecting window must be approximately 70°. It was

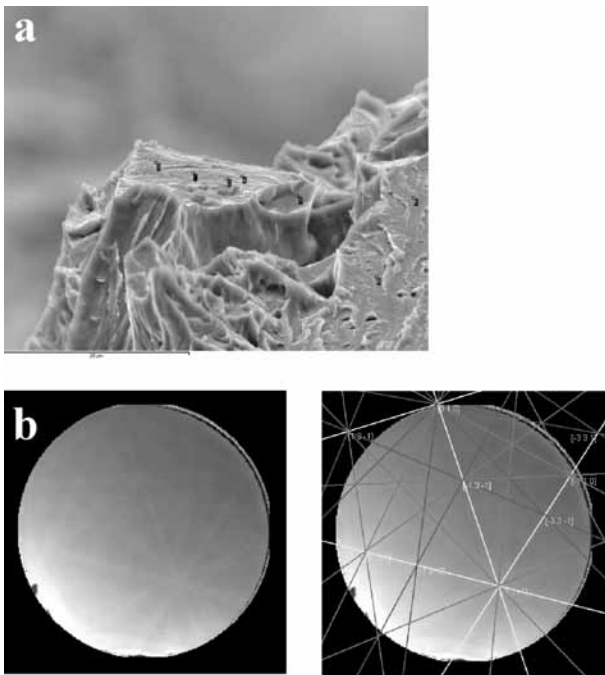


**Figure 9:** Specimen quenched in water from 1250 °C. Microstructure: coarse-grained martensite. Microfractography, diffraction lines, resolved diffraction lines and space-orientation indexes for the marked cleavage facet

**Slika 9:** Preizkušane, kaljen v vodi s 1250 °C. Mikrostruktura: grobozrnati martenzit. Mikrofraktografija, difrakcijske črte, razločene difrakcijske črte in indeksi prostorske lege za označeno cepilno ploskev

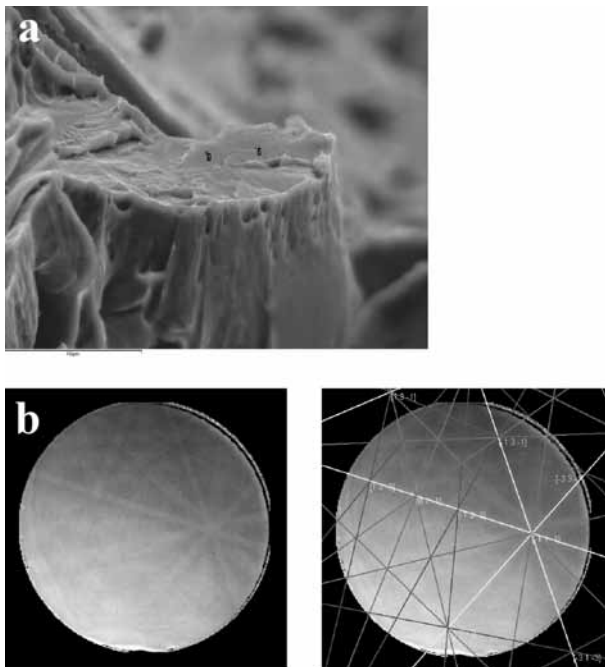


**Figure 10:** Specimen cooled in lead bath from 1250 °C. Microstructure: coarse-grained bainite. Microfractography, diffraction lines, resolved diffraction lines and space-orientation indexes for the marked cleavage facet

**Slika 10:** Preizkušane, ohlajen v svincu 1250 °C. Mikrostruktura: grobozrnati bainit. Mikrofraktografija, difrakcijske črte, razločene difrakcijske črte in indeksi prostorske lege za označeno cepilno ploskev

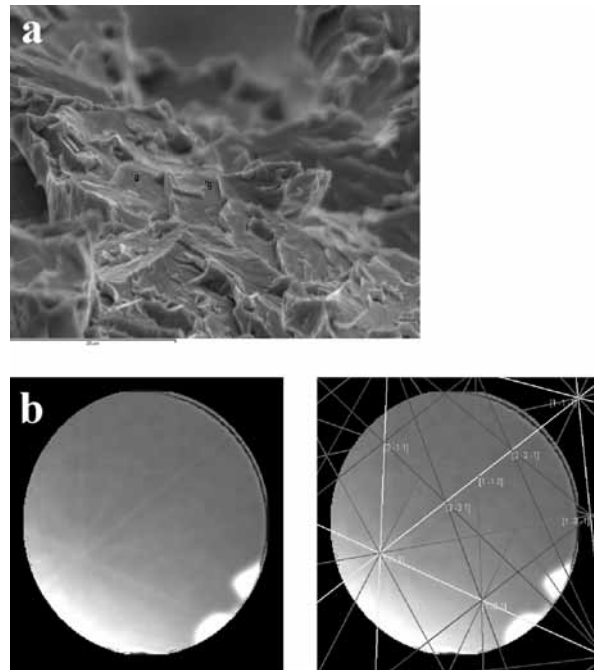


**Figure 11:** Specimen from fig. 9 reheated at 750 °C. Microfractography, diffraction lines, resolved diffraction lines and space-orientation indexes for the marked cleavage facet

**Slika 11:** Preizkušane, kaljen v vodi s 1250 °C in segreti pri 750 °C. Mikrostruktura: popuščeni grobozrnati martenzit in sekundarni martenzit. Mikrofraktografija, difrakcijske črte, razločene difrakcijske črte in indeksi prostorske lege za označeno cepilno ploskev

virtually impossible to obtain the required position of the cleavage facets on the rugged brittle fracture surface. For this reason, the diffraction did not produce the theoretical low orientation indexes characteristic for the spatial orientations (001) and (011), but high indexes with a marked difference in intensity approaching the (001) plane. In **Figures 9 and 10** the obtained diffraction lines and the computer identification of diffraction lines are shown for the fracture of martensite and bainite obtained with water and lead cooling from 1250 °C<sup>1</sup>. The indexes of the cleavage facets approach in all cases the (010) plane, while the vertical axis approaches the direction of (012). A virtually identical space orientation was obtained for cleavage facets on specimens which were reheated at 750 °C and air cooled (**Figure 11**). It is concluded that the microstructure does not affect the space orientation of the cleavage facets.

## 6 RELATION OF THE LEAVAGE STRENGTH AND THE CHARPY TOUGHNESS CHARACTERISTICS

In **Table 1** the date of the Charpy tests are given,<sup>1</sup> selected as characteristics for the comparison of the Charpy behaviour of the tested microstructure and their tensile characteristics as well as the cleavage strength. The experimental findings do not show a clear connection between the characteristics of both kinds of

testing. Also, these data do not indicate a relation between the brittle threshold temperature and the cleavage strength for the tested microstructures, although the assumption that the brittle fracture should occur at a higher temperature and with a lower cleavage strength seems to be logical. It is assumed that the eventual connection is probably masked by the effect of the diversity in the loading mode and the difference in the test rate of the Charpy notch toughness flexion test and the tensile test of the notched axial specimen at a much smaller deformation rate.

## 7 CONCLUDING REMARKS

The tensile tests of notched specimens of the same steel with an initial microstructure and a microstructure of quenched fine- and coarse-grained martensite and bainite and with the microstructure obtained with a short annealing in the two-phase – austenite + ferrite – region show that the brittle fracture, cleavage strength and the plastic extension before the fracture are not related to the hardness. Also, no connection was established between the tensile characteristics and the temperature of the cleavage fracture with the Charpy notch toughness tests.

The fracture of all but two specimens occurred after plastic deformation. While the yielding was found only for the specimens with the initial and reheated microstructures. The fracture surface of all the specimens consisted of a narrow ring of plastic shearing ahead of the notch tip and a central cleavage area.

The plane of the cleavage facets was (001) and this was independent of the microstructure and the plastic deformation before the fracture. The shearing ring was found on all the fractures, as well as on specimens fractured with a very low plastic deformation, and its width was greater with a greater plastic deformation. On all the specimens at least two shearing initials were formed at the notch tip that joined after a different extension, which may be related to the distance

necessary for the crack tip radius to decrease to a critical value characteristic for the microstructure.

The general conclusion is that all the relations between the tensile and Charpy characteristics for the same type of steel microstructure are masked by the difference in the specimen geometry and the test rate between the Charpy flexion test that occurs in  $0.01 \text{ s}^{-1}$  and the tensile test with a several orders of magnitude smaller rate.

The authors are indebted to the Ministry of Science and High Education of Slovenia for funding the project.

## 8 REFERENCES

- <sup>1</sup> G. Kosec, F. Vodopivec A. Smolej, J. Vojvodič Tuma. Steel Research, submitted for printing
- <sup>2</sup> F. Vodopivec, G. Kosec, S. Grbič, D. Kmetič: Mater. Tehnol. 38 (2004), 149
- <sup>3</sup> B. Ule, V. Leskovšek, B. Tuma: Eng. Fracture Mechanics 65 (2000), 559–572
- <sup>4</sup> C. Betegon, F. J. Belzunce, C. Rodriguez: Acta Materialia 33 (1996), 1055–1061
- <sup>5</sup> S. R. Bordet, A. D. Karstensen, D. M. Knowles, C. S. Wisner: Engineering Fracture Mechanics 72 (2005), 453–473
- <sup>6</sup> C. J. Esser, F. Grimpe, W. Dahl: Steel Research 66 (1995), 259–263
- <sup>7</sup> J. Vojvodič Tuma: Journal of Materials Processing Technology 121 (2002), 323–331
- <sup>8</sup> F. Vodopivec, B. Breskvar, B. Arzenšek, D. Kmetič, J. Vojvodič Tuma: Mat. Sci. Techn. 18 (2002), 61–67
- <sup>9</sup> P. W. Bridgeman: Studies in Large Plastic Flow and Fracture; McGraw-Hill New York, 1952, p. 9. Loc cit. Ref. 12
- <sup>10</sup> H. Kurishita, H. Nayano, M. Narui, M. Yamazaki, Y. Kano, I. Shibahara: Mater. Trans. JIM, 34 (1993), 1042–1052
- <sup>11</sup> F. Vodopivec, B. Arzenšek, D. Kmetič, J. Vojvodič Tuma: Mater. Tehnol. 37 (2003), 317–326
- <sup>12</sup> J. F. Knott: Met. Sci. 14 (1980), 327–336
- <sup>13</sup> D. A. Curry: Met. Sci. 14 (1980), 319–326
- <sup>14</sup> R. Sandström, Y. Bergson Met. Sci 18 (1984), 177–186
- <sup>15</sup> D. A. Curry, J. F. Knott: Met. Sci. 10 (1976), 1–6
- <sup>16</sup> S. T. Mandziej: Metall. Trans. A 24A (1993), 545–552
- <sup>17</sup> F. Vodopivec, L. Kosec B. Breskvar: Metalurgija 39 (2003), 139–140